Seventh International Conference on Computational Fluid Dynamics (ICCFD7), Big Island, Hawaii, July 9-13, 2012

ICCFD7-4004

Three-dimensional Phenomenon of Continuously Rotating Detonation Engines

Rui Zhou *, Jian-ping Wang * and Dan Wu *
Corresponding author: ameliazhr@163.com

*State Key Laboratory of Turbulence and Complex System, Department of Mechanics and Aerospace Engineering, College of Engineering, Peking University, Beijing, China.

Abstract: The effect of chamber depth on the continuously rotating detonation engines(RDE) flow field is discussed. The results demonstrate that the radial dimension is not obvious when the chamber depth is small. However when the chamber depth is 10mm or 14mm, the radial dimensional phenomenon is more and more obvious. At the head wall, shock waves reflect repeatedly between the inner wall and outer wall. Both regular reflection and mach reflection exist at the head wall. The length of mach stem increases as the chamber depth is increased. The maximum pressure and thrust linearly increases with increasing the chamber depth. The detonation height and specific impulse are shown to be nearly constant as the chamber depth is increased.

Keywords: RDE, Numerical Simulation, Three-dimensional Phenomenon, Shock Wave Reflection.

1 Introduction

Detonation is a shock-induced combustion process in which the energy from the combustion release supports the shock to propagate. The shock compresses the mixture to initiate the detonation and provides it with energy to be self-sustained [1]. In terms of propulsive applications, a detonation-based engine has higher propulsive efficiency, wider operating ranges from low subsonic to high supersonic speed, and simpler and more compact combustor designs [2]. The most common type of a detonation-based propulsion system is pulse detonation engines (PDE). But there are several hurdles that need to be overcome in the PDE research [2,3]. There have been alternative attempts to use detonation combustion into a propulsion system, called rotating detonation engines (RDE).

The basic phenomenon of the RDE have been experimentally and theoretically investigated by Bykovskii et al. [4], followed by the pioneering works of Voitsekhovskii [5] and Nicholls et al. [6]. Wolanski et al. [7] achieved experimentally the rotating detonation in a coaxial combustion chamber where the detonation velocity was close to the Chapman-Jouguet value. They also obtained the range of propagation stability as a function of chamber pressure, composition, and geometry [8]. In the numerical simulation aspect, Zhdan et al. [9] performed two-dimensional unsteady modeling of the rotating detonation in an annular chamber with a hydrogen-oxygen mixture, and Davidenko et al. [10] simulated the rotating detonation with the detailed kinetic model of a hydrogen and oxygen mixture. Recently, Hishida et al. [11] numerically studied the detailed flow field structure of the rotating detonation with the two-step chemistry of an argon-diluted hydrogen and oxygen mixture. Tae-Hyeong et al. [12] investigated the influence of various design parameters on the propulsive

performance where parametric variables include total pressure, total temperature, injection area ratio, axial chamber length and the number of detonation waves. Shao et al. [13,14] comprehensively studied three-dimensional (3D) numerical simulations in the RDE. They obtained multi-cycles of the rotating detonation, and discussed several key issues, including the fuel injection limit, self-ignition, thrust performance and nozzle effects.

In the numerical investigation of RDE, most researchers assume that the distance between the two coaxial cylinders is much smaller than their diameters and axial length, so the flow field can be approximated as a two-dimensional (2D) plane without thickness along the radial direction [12]. The difference of the flow field within the RDE along the radial direction has never been investigated. In present work, the radial dimensional phenomenon of the flow field within the RDE is investigated in the coaxial annulus combustion chamber. At the head end, shock waves repeatedly reflect between the inner wall and the outer wall. We find that both the regular reflection and the mach reflection exist at the head end. The Mach stem will be different because of the different chamber geometry. Through this research, the 3D flow field structure of the RDE can be better understood, and the numerical results can provide basis for the explanation of experimental results.

2 Numerical Method and Physical Modeling

Three-dimensional Euler equations with chemical reaction are used as governing equations. A one-step chemical reaction model of stoichiometric hydrogen/air is used. Viscosity, thermal conduction and mass diffusion are ignored.

The governing equations in the calculated coordinates as follows:

$$\frac{\partial \boldsymbol{U}}{\partial t}+\frac{\partial \boldsymbol{E}}{\partial \xi}+\frac{\partial \boldsymbol{F}}{\partial \eta}+\frac{\partial \boldsymbol{G}}{\partial \zeta}=\boldsymbol{S}$$

where the dependent variable vector $\boldsymbol{U}$, convective flux vectors $\boldsymbol{E}$, $\boldsymbol{F}$ and $\boldsymbol{G}$, and source vector $\boldsymbol{S}$ are defined as

$$\boldsymbol{U}=\frac{1}{J}[\rho \ \ \rho u \ \ \rho v \ \ \rho w \ \ e \ \ \rho\beta]^{\mathrm{T}}$$

$$\begin{aligned}\boldsymbol{E}=[&\rho\bar{U} \ \ \rho\bar{U}u+p\xi_x \ \ \rho\bar{U}v+p\xi_y \ \ \rho\bar{U}w+p\xi_z\\ &\bar{U}(p+e) \ \ \rho\bar{U}\beta]^{\mathrm{T}}\end{aligned}$$

$$\begin{aligned}\boldsymbol{F}=[&\rho\bar{V} \ \ \rho\bar{V}u+p\eta_x \ \ \rho\bar{V}v+p\eta_y \ \ \rho\bar{V}w+p\eta_z\\ &\bar{V}(p+e) \ \ \rho\bar{V}\beta]^{\mathrm{T}}\end{aligned}$$

$$\begin{aligned}\boldsymbol{G}=[&\rho\bar{W} \ \ \rho\bar{W}u+p\zeta_x \ \ \rho\bar{W}v+p\zeta_y \ \ \rho\bar{W}w+p\zeta_z\\ &\bar{W}(p+e) \ \ \rho\bar{W}\beta]^{\mathrm{T}}\end{aligned}$$

$$\boldsymbol{S}=\frac{1}{J}[0 \ \ 0 \ \ 0 \ \ 0 \ \ 0 \ \ \rho\dot{\omega}_\beta]^{\mathrm{T}}$$

$$\bar{U}=u\xi_x+v\xi_y+w\xi_z$$

$$\bar{V}=u\eta_x+v\eta_y+w\eta_z$$

$$\bar{W}=u\zeta_x+v\zeta_y+w\zeta_z$$

The pressure p and total energy e are calculated by using equations of state:

$$p=\rho RT$$

$$e=\frac{p}{\gamma-1}+\beta\rho q+\frac{1}{2}\rho(u^2+v^2+w^2)$$

where ρ is density, R gas constant, T temperature, γ specific heat ratio and q heat release per

unit mass. The mass production rate is:

$$\dot{\omega}_\beta = \frac{d\beta}{dt} = -A\beta \exp(-E_a/(RT))$$

where β is the mass proportion of reaction mixture gas, A preexponential factor and E_a activation energy per unit mass. A detailed description of all the parameters can be found in [15]. Flux terms are solved by using 5-order MPWENO scheme [16], and the time integration is performed by using 3-order TVD Runge-Kutta method. The grid size is 0.2mm along the radial and the axial direction. The grid number is 800 along the azimuthal direction. The grid dependency has been validated in [14].
The combustion chamber of the RDE is a coaxial cavity with a toroidal section in Fig.1. A detonation wave propagates azimuthally in the annular chamber while a combustible mixture is injected from the head end, and then the burnt gas spurts out of the downstream exit. At the head end, there are a large number of Laval micro-nozzles to axially inject premixed hydrogen/air gas into the combustion chamber. The mass flux of the incoming fuel is controlled by the relationship between the inlet stagnation pressure and flow pressures at the head end.

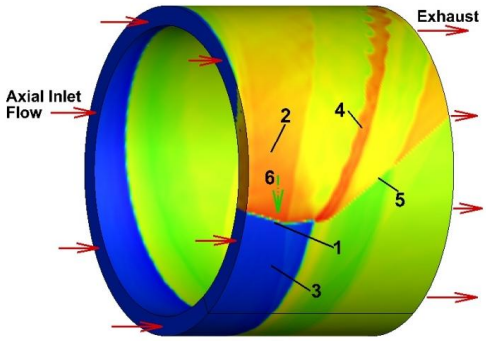

Fig.1 RDE propagation schematic structure. 1- detonation wave, 2- burnt product, 3- fresh premixed gas, 4- contact surface, 5- oblique shock wave, 6- detonation wave propagation direction.

The flow field is initially filled with quiescent, combustible products mixture at pressure 0.101MPa and temperature 300K. A one-dimensional C-J detonation wave is distributed in a limited region near the head end in order to initiate the stoichiometric hydrogen/air gas mixture. The injection boundary condition is specified according to [14]. A rigid wall condition is used at the inner wall and the outer wall. Boundary conditions on the outflow boundary correspond to a non-reflecting surface.

3 Results and Discussion

The numerical simulation is performed in three different combustion chambers whose chamber depth is 4mm, 10mm and 14mm respectively. The chamber length is 4.8cm, and the inner radius is 3 cm. the inlet stagnation pressure is 3MPa and the environment pressure is 0.05MPa. Fig. 2 shows the pressure and the temperature contours after the detonation propagating stably. When the chamber depth is $\Delta = 10\text{mm}$ and $\Delta = 14\text{mm}$, it is seen clearly that there is shock wave reflection repeatedly between the inner wall and the outer wall near the head end. The form of shock wave reflection is not only limited to the regular reflection, but also the mach reflection exists at the inner wall. The length of mach stem increases as the chamber depth is increased. The maximum pressure in the whole flow field increases as the chamber depth increasing.

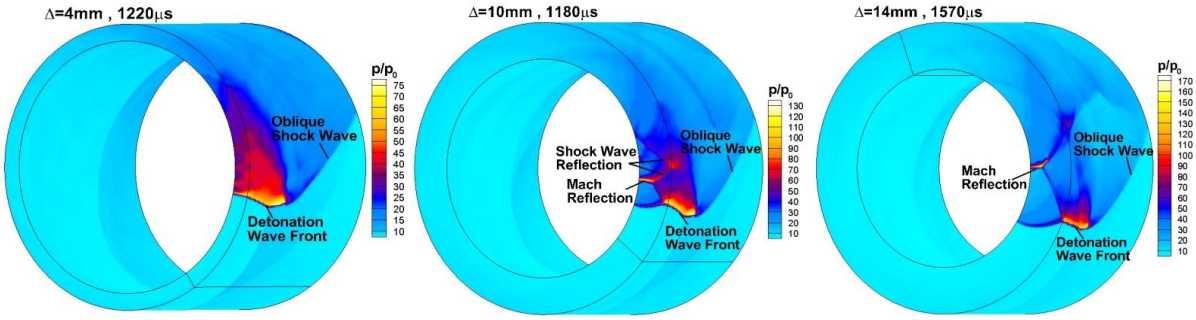

(a) Pressure contour as the chamber depth increasing.

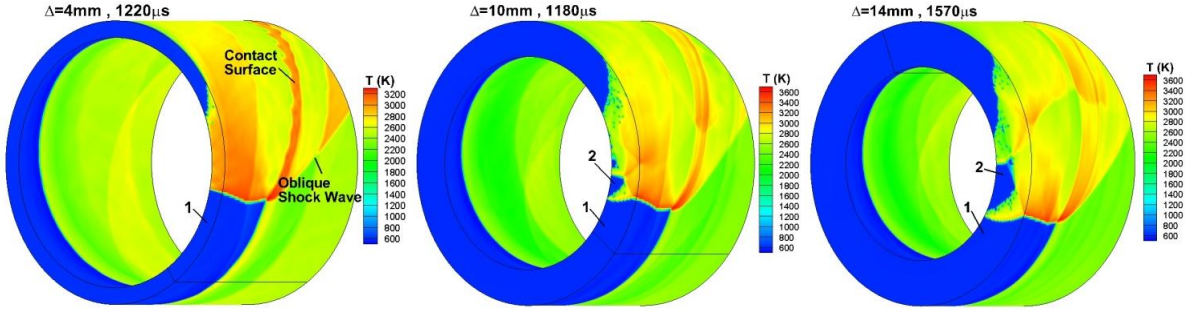

(b) Temperature contour as the chamber depth increasing.

Fig. 2 Pressure (a) and temperature(b) contour when the chamber depth is 4mm, 10mm, and 14mm.

We extend the annulus of the combustion chamber to a two-dimensional plane in order to analyzing clearly the flow field variation along the radial direction. Fig. 3 shows the pressure contour on the inner annulus, the middle annulus and the outer annulus of the combustion chamber after the detonation propagates stably in the three chamber geometries. Fig. 3 (a) shows that the difference of flow field along radial direction is not obvious when the chamber depth $\Delta = 4\text{mm}$ is small. The maximum pressure increases with the radius of annulus increasing. The difference of flow field is more and more obvious along the radial direction when the chamber depth increases that is $\Delta = 10\text{mm}$ and $\Delta = 14\text{mm}$, as shown in Fig. 3 (b) and (c). The flow field shows total different wave characteristics on the inner annulus, the middle annulus and the outer annulus. The maximum pressure on the outer annular is highest, and then on the inner annular, the maximum pressure on the middle annular is lowest. Fig. 3 (b) and (c) show that there are two strong waves on the inner annulus. One is the detonation front, and the other exists because of the mach reflection. At the front of the mach stem the pressure decreases because of the mach reflection, so a little fresh gas can be injected into the combustion chamber (as shown domain 2 in Fig. 2 (b)), and then it is burned rapidly. The pressure and the temperature increase at the mach stem, so the second wave is stronger than the detonation wave on the inner wall.

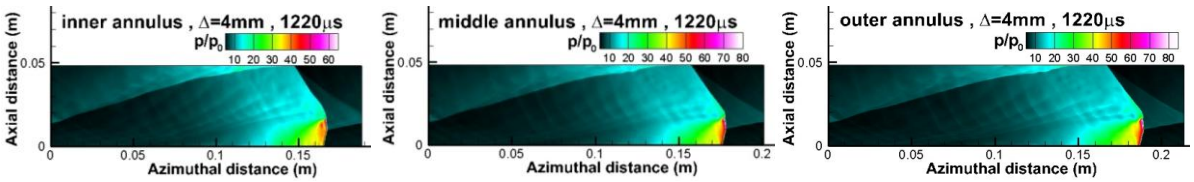

(a) Chamber depth is 4mm.

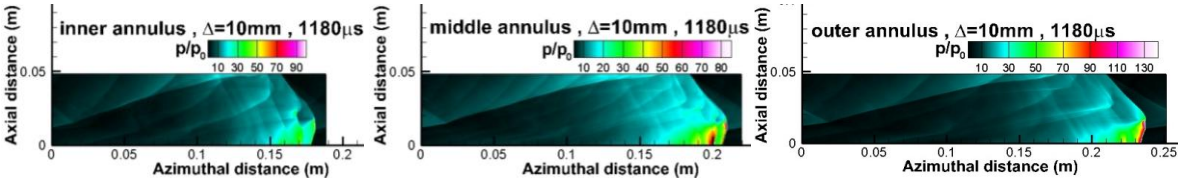

(b) Chamber depth is 10mm.

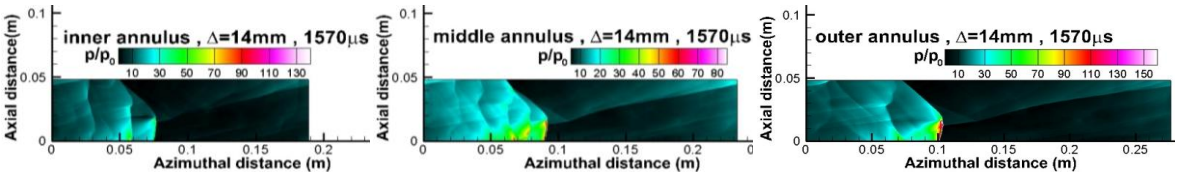

(C) Chamber depth is 14mm.

Fig. 3 Pressure distribution at the inner annulus, middle annulus and outer annulus as the chamber depth increases.

Fig. 4 shows the influence of the chamber depth on detonation height h and maximum pressure (a), thrust and specific impulse (b). The maximum pressure and the thrust linearly increase with increasing the chamber depth. The detonation height and the fuel-based gross specific impulse are shown to be nearly constant as the chamber depth is increased. When the chamber depth is 14mm, the disturbance of the specific impulse is larger than that when the chamber depth is 4mm or 10mm after detonation propagating stably. When the initial conditions are the same, the detonation wave need longer time to propagation stably with the chamber depth increasing.

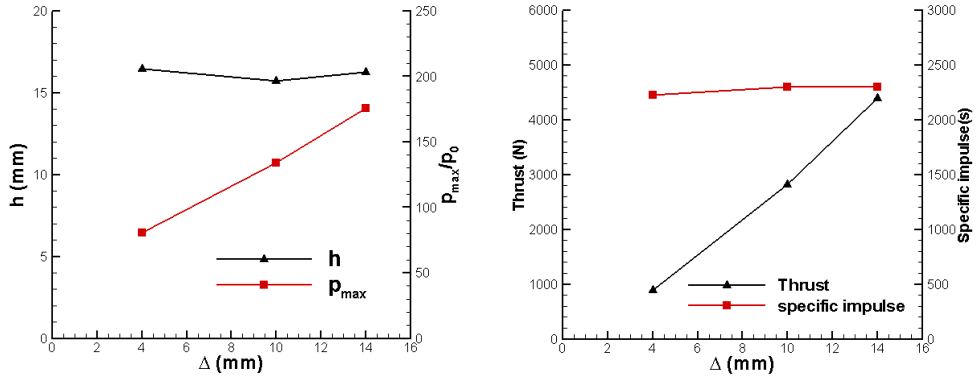

(a) Detonation height and maximum pressure (b) Thrust and specific impluse

Fig. 4 Several parameters variation as the chamber depth increasing.

4 Conclusions

Shock waves reflect repeatedly between the inner wall and the outer wall near the head end. The form of shock wave reflection is not only limited to the regular reflection, but also the mach reflection exists at the inner wall. The length of mach stem increases as the chamber depth is increased. The maximum pressure and thrust linearly increases with increasing the chamber depth. The detonation height and specific impulse are shown to be nearly constant as the chamber depth is increased. When the initial conditions are the same, the detonation wave need longer time to propagation stably with the chamber depth increasing.

References

[1] Mahmoudi, Y., Mazaheri, K.: High resolution numerical simulation of the structure of 2-D

gaseous detonations. Proceedings of the Combustion Institute 33, 2187-2194 (2011).
[2] Roy, G.D., Frolov, S.M., Borisov, A.A., Netzer, D.W.: Pulse detonation propulsion: challenges, current status, and future perspective. Progress in Energy and Combustion Science 30(6), 545-672 (2004).
[3] Li, Q., Fan, W., Yan, C.J.: Experimental investigation on performance of pulse detonation rocket engine model. Chinese Journal of Aeronautics 17(1), 9-14 (2004).
[4] Bykovskii, F.A., Zhdan, S.A., Vedernikov, E.F.: Continuous spin detonation. Journal of propulsion and power 22(6), 1204-1216 (2006).
[5] Voitsekhovskii, B.V., Soviet, J.: Stationary spin detonation. Soviet Journal of Applied Mechanics and Technical Physics 3, 157-164 (1960).
[6] Nicholls, J.A., Cullen, R.E., Raglano, K. W.: Feasibility studies of a rotating detonation wave rocket motor. Journal of Spacecraft and Rockets 3(6), 893-898 (1966).
[7] Wolanski, P., Kindracki, J., Fujiwara, T.: An experimental study of small rotating detonation engine. Pulsed and Continuous Detonations, edited by Roy, G.D., Frolov, S.M., and Sinibali, J., Torus Press, Moscow, 332-338 (2006).
[8] Kindracki, J., Wolanski, P., Gut, Z.: Experimental research on the ratating detonation in gaseous fuels-oxygen mixtures, Shock Waves 21, 75-84 (2011).
[9] Zhdan, S.A., Bykovskii, F.A., Vedernikov, E.F.: Mathematical modeling of a rotating detonation wave in a hydrogen-oxygen mixture. Combustion, Explosion and Shock Waves 43(4), 449-459 (2007).
[10] Davidenko, D.M., Gokalp, I., Kudryavtsev, A.N.: Numerical study of the continuous detonation wave rocket engine. AIAA Paper 2008-2680, 15th AIAA International Space Planes and Hypersonic Systems and Technologies Conference, Dayton, Ohio 2008.
[11] Hishida, M., Fujiwara, T., Wolanski, P.: Fundamentals of rotating detonation. Shock waves 19(1), 1-10 (2009).
[12] Tae-Hyeong Yi, Jing Lou, Cary Turangan, Choi, J.Y., Wolanski, P.: Propulsive performance of a continuously rotating detonation engine. Journal of Propulsion and Power 27(1), 171-181 (2011).
[13] Shao, Y.T. and Wang, J.P.: Change in Continuous Detonation Wave Propagation Mode from Rotating Detonation to Standing Detonation, Chinese Physics Letters 27(3), 034705 (2010).
[14] Shao, Y.T., Wang, J.P.: Continuous Detonation Engine and Effects of Different Types of Nozzle on Its Propulsion Performance. Chinese Journal of Aeronautics 23(6), 647-652 (2010).
[15] Ma, F.H., Choi, J.Y., Yang, V.G.: Propulsive performance of airbreathing pulse detonation engines. Journal of Propulsion and Power 22(6), 1188-1203 (2006).
[16] Balsara, D.S., Shu, C.W.: Monotonicity preserving weighted essentially non-oscillatory schemes with increasingly high order of accuracy. Journal of Computational Physics 160(2), 405-452 (2000).